# Flexible, Highly Sensitive Paper-Based Screen Printed MWCNT/PDMS Composite Breath Sensor for Human Respiration Monitoring

K. Thiyagarajan, *Student Member, IEEE*, G. K. Rajini, *Member, IEEE*, and Debashis Maji, *Member, IEEE*

***Abstract*—Accurate measurement and monitoring of respiration is vital in patients affected by severe acute respiratory syndrome coronavirus – 2 (SARS-CoV-2). Patients with severe chronic diseases and pneumonia need continuous respiration monitoring and oxygenation support. Existing respiratory sensing techniques require direct contact with the human body along with expensive and heavy Holter monitors for continuous real-time monitoring. In this work, we propose a low-cost, non-invasive and reliable paper-based wearable screen printed sensor for human respiration monitoring as an effective alternative of existing sensing systems. The proposed sensor was fabricated using traditional screen printing of multi-walled carbon nanotubes (MWCNTs) and polydimethylsiloxane (PDMS) composite based interdigitated electrodes on paper substrate. The paper substrate was used as humidity sensing material of the sensor. The hygroscopic nature of paper during inhalation and exhalation causes a change in dielectric constant, which in turn changes the capacitance of the sensor. The composite interdigitated electrode configuration exhibited better response times with a rise time of 1.178s being recorded during exhalation and fall time of 0.88s during inhalation periods. The respiration rate of sensor was successfully examined under various breathing conditions such as normal breathing, deep breathing, workout, oral breathing, nasal breathing, fast breathing and slow breathing by employing it in a wearable mask, a mandatory wearable product during the current COVID-19 pandemic situation.Thus, the above proposed sensor may hold tremendous potential in wearable/flexible healthcare technology with good sensitivity, stability, biodegradability and flexibility at this time of need.**

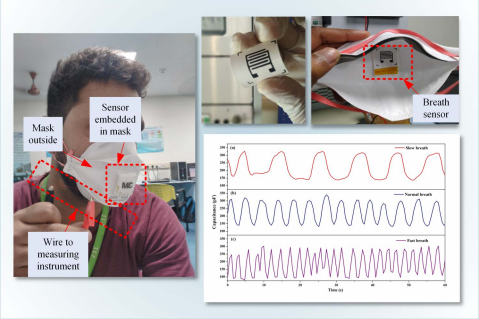


***Index Terms*—Multi-walled carbon nanotubes (MWCNT), polydimethylsiloxane (PDMS), MWCNT/PDMS composites, breath sensor, COVID-19, flexible sensor, humidity sensor.**

## I. Introduction

THE use of flexible and conformal sensors has seen an upsurge in wearable monitoring systems recently [1]. Flexible sensors have been opening up many new possibilities including non-invasive continuous real-time monitoring with high-level of comfort to the patients [2], [3]. The measurements of four primary physiological parameters namely body temperature [4], blood pressure [5], pulse rate [6] and respiration rate [7] are essential to assess the health condition of a person. Respiration rate holds a significant role among the four and is often regarded as a better performance parameter to distinguish various clinical patients[8], [9]. Any deviations from the normal breath rate of 12–20 times per minute may be caused due to the vivid clinical conditions like asthma, pneumonia, anaemia, cardiac arrest, etc [10], [11]. Therefore, it is imperative to have a continuous human respiration monitoring system to detect clinical patients.

Respiration rate, better known as respiration frequency can be measured both by contact or non-contact based methods. Contact based sensing approaches are most commonly used for respiration rate monitoring. In contact based, sensing elements are in touch with human body for measuring airflow rate [12], air temperature [13], chest wall movements [14], [15], air components [16], cardiac activity [17] and breathing sounds [18]. Measurement of airflow rate is the most widely used method in clinical practices. It is typically through the deployment of nasal or oronasal sensor which

Manuscript received September 26, 2020; revised November 12, 2020, November 16, 2020, and November 17, 2020; accepted November 17, 2020. Date of publication November 27, 2020; date of current version June 30, 2021. The associate editor coordinating the review of this article and approving it for publication was Dr. Calogero Maria Oddo. *(Corresponding author: G. K. Rajini.)*

K. Thiyagarajan and G. K. Rajini are with the School of Electrical Engineering, Vellore Institute of Technology, Vellore 632 014, India (e-mail: thiyagarajreddy@gmail.com; rajini.gk@vit.ac.in).

Debashis Maji is with the Department of Sensor and Biomedical Technology, School of Electronics Engineering, Vellore Institute of Technology, Vellore 632 014, India (e-mail: debashis.maji@vit.ac.in).

Digital Object Identifier 10.1109/JSEN.2020.3040995

detects the temperature change during inhalation and exhalation periods. However, there are some limitations associated with this technique due to occurrence of temperature sensor dislocations [19]. The use of pressure sensor is another option for airflow measurements based on the volume of exhaled air. But, the use of heavy and non-flexible mask often leads to discomfort for the patients [20]. Other available forms of measuring airflow include the thorax three-dimensional movement sensing and strain sensing of chest wall activity. But, they are highly sensitive to the non-breathing associated movements[21]. Besides, despite the functionality of traditional monitoring systems, they still poses portability and cost challenges. Hence, the design of innovative flexible sensors for real-time respiration monitoring has enormous prospects in wide range of applications.

A substantiate change of concentration of water molecules takes place during the respiration process. The drop in local relative humidity (RH) during inhalation due to the air flow taking away the water vapour and a subsequent rise in local relative humidity during exhalation due to the increased outflow of water vapour in the breath happens while respiration, irrespective of the relative humidity of the environment. Therefore, relative humidity sensor based respiration monitoring is less affected by the environmental conditions as compared to the mechanical sensors, conventional air flow meters and thermal sensors [22]. Relative humidity (RH) sensors are widely preferred because of its excellent accuracy, sensitivity, linearity and long-term operation. RH sensors work on the amount of change of water vapour content between inhaled and exhaled air near the substrate and tracks the data of the respiration rate. Many research studies have been performed to date regarding development of RH sensors to monitor respiration. Some of the research articles reported on humidity based respiratory sensors have used sophisticated techniques using carbon materials [23], [24], metal oxide [25], transition metal dichalcogenide [26], etc., which are not only expensive, but also poses difficulties for large scale fabrication. Other issues related to such sensors synthesized on flexible substrates such as polydimethylsiloxane, polyimide, polymerized ionic liquids and plastic are non-porous, non-disposable and partial bio-compatibility. Further, Li et al reported silk based humidity sensors which require complex fabrication process and lack flexibility and comfortability [27]. Very recently, Xie *et al.*also fabricated leather based respiration sensor [28]. However, although leather is preferred as a flexible substrate with better hygroscopicity and porosity, they often tend to cause allergies and discomfort. These pertaining issues compel research community to explore novel green processing of environment-friendly materials in respiration monitoring.

Screen printing process is a popular method among various traditional processes such as inkjet, screen and gravure. These methods can be applied for large-area, lightweight, low-cost, flexible electronic devices, biocompatible, electrochemical sensors, pressure sensors, enzymatic biosensors, strain gauge, organic thin-film transistors (OTFTs) and active-matrix displays [29]–[31]. Other advantages of screen printing are its ability to print large areas and economic viability of the process. It can also be effectively applied to various substrates such as ceramic, plastic, textiles, glass and paper [32]. Recently, paper based sensors has proved to be of significant potential owing to their characteristics like low cost and investment, flexibility, light weight, disposability, biocompatibility, etc [33]. Many of these concepts were shown on wearable paper based sensors including biosensor [34], strain sensor [35], [36] pressure sensor [37] and and temperature sensor[38]. Successful developments of these sensors show high potential for paper-based sensors in wearable technology. The paper sensor is also able to convert any changes in moisture level to electric signal. Gider *et al.* fabricated the paper-based humidity sensor for respiration monitoring via digital printing of carbon ink [39]. Kanaparthi *et al.* utilized the direct drawing of electrode with pencil on paper to realize a respiration sensor [40]. Duan *et al.* presented a humidity sensor with polyester conductive adhesive tape electrode to promote flexibility [40]. However, there are problems to be addressed in practical realization of the above paper-based sensors. First, the fabricated sensor electrodes are prone to cracking when the paper is folded multiple times which limits its flexibility and the carbon materials used are also well sensitive towards humidity levels which limits the response of the sensors [39], [40]. Second, the fabrication technology involved in the above work such as digital printing of electrodes [39] has limited flexibility and is expensive. Third, the pencil drawn and conductive adhesive tape electrodes methods of fabrication are not appropriate towards the rapid production and shows variation in repeatability and reproducibility [40], [41]. Therefore, developing a facile fabricating method and choosing a suitable flexible and humidity insensitive electrode material for enhancing the performance of the paper-based humidity sensors are challenging and highly necessary.

In this work, we report an efficient and cost-effective respiration sensor developed using MWCNT/PDMS composite materials on a paper surfaces for clinical applications. PDMS has high flexibility, good chemical and thermal stability and biocompatibility with easy fabrication steps which makes it a popular choice for realizing bio-flexible devices [42]. In addition, CNTs have also been a popular choice for sensors and wearable devices due to its tunable electrical, mechanical and sensing properties [43], [44]. Screen printing technique was used for coating MWCNT/PDMS composite interdigitated electrode over a paper substrate and silver glue for contact territory on the same. The sensor was studied under different breathing situations (e.g., normal breath, deep breathing, nasal and oral breath) as well as analyzed for respiration rate, breathing intervals and breathing index. The sensor was capable of measuring and distinguishing different breathing conditions thus reporting the realization of a simple, inexpensive, highly sensitive, facile to fabricate large quantity sensors for respiration monitoring.

## II. Experiment

In the present work a novel nanocomposite based on multi-walled carbon nanotubes (MWCNT) and polydimethylsiloxane (PDMS) is used to develop a capacitive humidity sensor using screen printing technique for the application of respiration measurements. The carbon-based nano-filler, CNTs

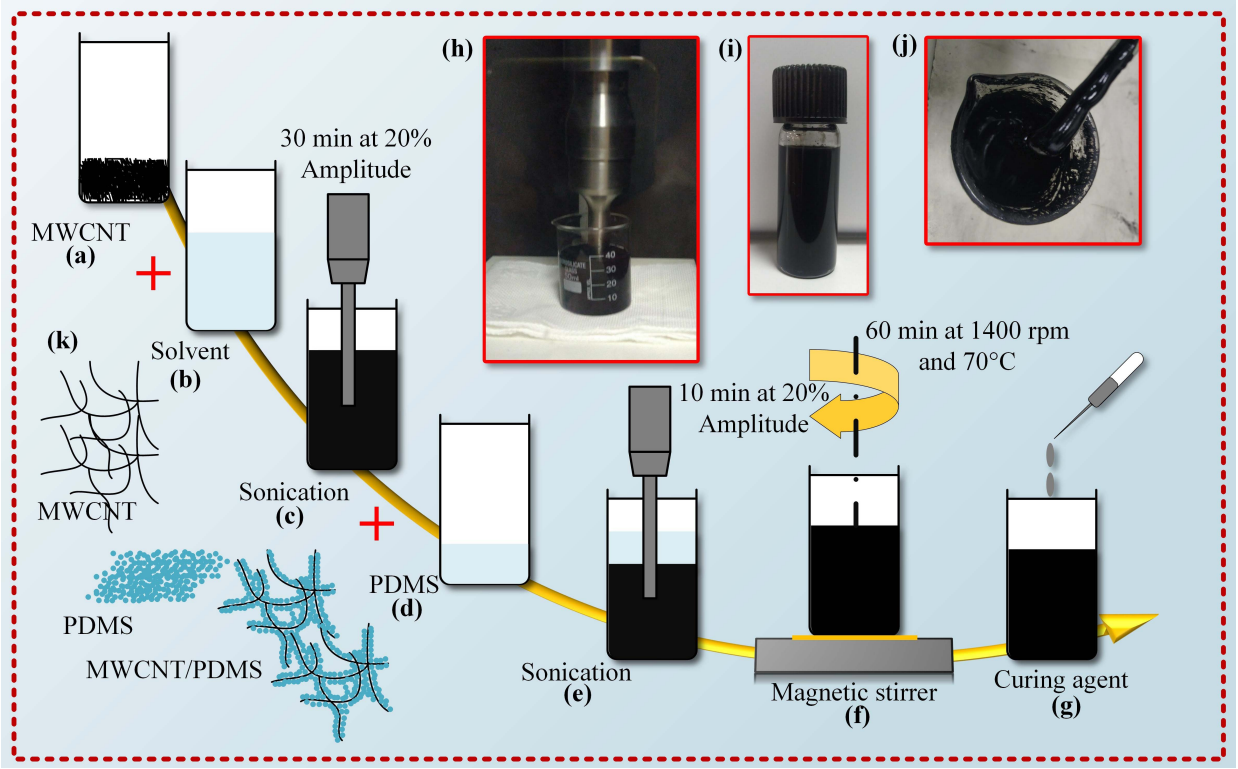


Fig. 1. (a-g) A schematic illustrating the preparation of MWCNT-PDMS composite; (h-i) Prepared MWCNT-PDMS composite; (j) Stable dispersion of MWCNT in THF; (k) Schematic illustration of composite.

improves mechanical, electrical and thermal conductivity of polymer composites, owing to their inherent properties such as a high aspect ratio, superior elastic modulus, and high conductivity showing good electron transfer property. Also, conductive polymers possess analogous characteristics to metals and inorganic semiconductors, but the same time maintains the polymer properties such as flexibility, easy processing capabilities, and synthesis leading to the rapid utilization of MWNT/PDMS nanocomposites in realization of various sensors and actuators [44], [45].

### *A. Composite Synthesis*

The polymer based elastomeric composite was prepared by dispersion of different concentrations of conductive MWCNT in non-conductive PDMS. Their consistent dispersion still remains a significant problem for many researchers. Magnetic stirring and probe sonication methods are generally used to optimize the dispersion of MWCNTs in PDMS by solvent dispersion technique. Effective dispersion of MWCNT filler in highly viscous PDMS elastomer requires enough energy. To attain this, an organic solvent THF, known as precursor for polymers is being used to pre-disperse the MWCNT and then mixed into PDMS subsequently. Three various solution samples, having 1%, 3%,5% and 6% as weight ratios of MWCNT in PDMS, are prepared to verify the screen printability of the MWCNT/PDMS composite solution. MWCNTs with dimension 10$\mu$m length and 5-20nm outer diameter are initially dispersed into the 30 ml of THF solution using a 13 mm probe sonicator from Sonics VCX 750 for 30 mins at 20% amplitude. After uniform dispersion of nanotubes in THF as shown in Fig.1(i), 5 grams of PDMS base was mixed with the CNT dispersed solution and kept again for ultrasonication for 10 min at 20% amplitude. The resulting mixture was thereafter kept over a magnetic stirrer and stirred for 60 min at 1400 rpm and heated at 70°C. Magnetic stirring aided in achieving consistent distribution of the MWCNT in PDMS with almost 80% of THF evaporating and leaving only MWCNT in the PDMS base matrix. Cross-linking agent was subsequently included to the base solution in 1:10 ratio after it was allowed to cool for 8 hours. The blend of nano composite and curing agent was mixed manually for 15 min thereafter and placed at 2°C in a refrigerator for preservation. Similar procedures were followed for developing all the three solution samples. The self-life of the nano composite was observed to be up to 120 days. Fig. 1(a)–(g) illustrates the schematic presentation of the complete composite preparation.

Although direct biocompatibility studies of the fabricated breath sensor was not conducted, previous literatures may support its possible usage with skin mounted wearable devices showing no skin redness upto 7 days of wearing as composites [44], [46]. Moreover, probe sonication method used for dispersing MWCNTs is expected to reduce the metallic impurities in MWCNTs and when embedded deep into the polymerized PDMS matrix as a composite may be further suitable for external usage [44], [46] as an initial feasibility study. In this context, necessary laboratory precautions need to be maintained while processing MWCNTs for similar sensing applications and further studies requires to be done to completely access the safety and biocom-

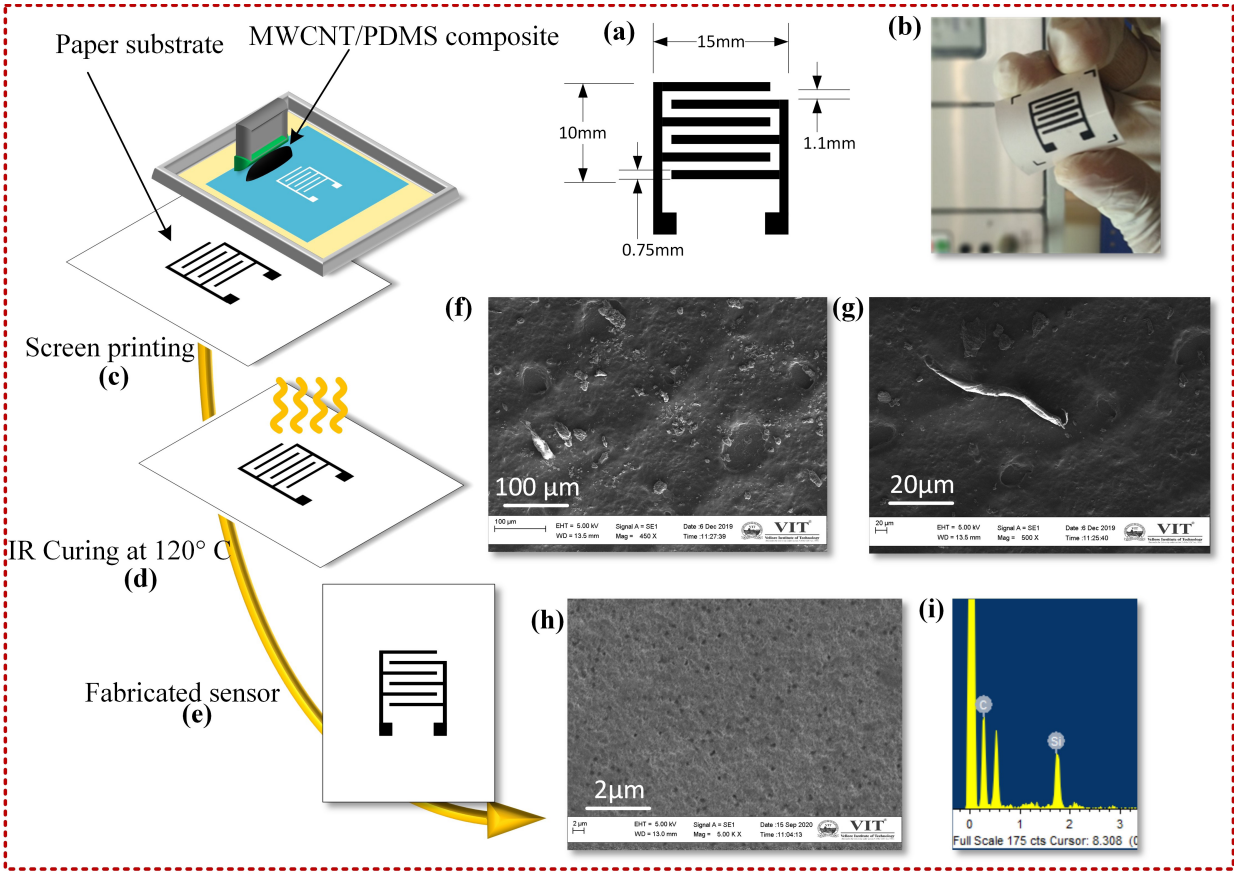


Fig. 2. (a) Sensor geometrical dimension; (b) fabricated sensor; (c-e) Paper base humidity sensor fabrication process; (f-g) SEM image of composite; (h) SEM image of paper substrate; (i) EDX analysis of composite.

patibility of these devices before it can be made into a commercially viable product.

### B. Sensor Design and Fabrication

The fabrication of the paper-based breath sensor comprises three steps: design of sensor, photo mask preparation for screen printing and printing the MWCNT/PDMS composite over the paper substrate and drying. An interdigitated electrode (IDE) pattern is selected, which enables the quick access of humid air to the paper and increases the sensitivity due to increased surface area. The interdigitated capacitive sensor is preferable to resistive sensor owing to less sensitive to bending strain and temperature. The capacitance (C) of the interdigitated electrode sensor is given by Equ.1 [47].

$$C = L(N-1)\left[\frac{\epsilon_0\epsilon_{r,t}}{2}\frac{K\left[(1-k^2)^{\frac{1}{2}}\right]}{K(k)} + 2\epsilon_0\epsilon_{r,m}\frac{t}{s}\right] \quad (1)$$

where C represents the capacitance of the IDE structure, L indicates the length of each electrode fingers and N is the number of unit cells $\epsilon_0$ denotes the permittivity of vacuum and is given by $8.851 \times 10^{12}$ As/Vm and $\epsilon_{r,t}$ is the relative permittivity surrounding the electrodes. $\epsilon_{r,m}$ is the relative permittivity between the electrodes and represents the capacitance due to the transverse field. K(k) denotes the elliptical integral of first order to calculate the impact of the fringing field sideways. The modulus k is given by the periodic arrangement of the electrodes and is expressed as shown in Equ.2.

$$k = cos\ (\frac{\pi}{2}\frac{w}{s+w}) \quad (2)$$

The parameters t, s, and w indicate the electrode thickness, electrode interspacing and width of electrode fingers, respectively. The electrode gap distance as an important factor affecting humidity sensing in paper-based humidity sensor, with the increase of the electrode distance the response of the humidity sensor progressively $\epsilon_0$ decreases as per the previous report. Considering the humidity sensing performance of the sensor and the accuracy of the manual printing process, an electrode distance of 1mm was selected. The geometries are designed with 15 mm × 10 mm as the active sensing area. The distance between the electrodes is 1.1 mm and width of each electrode, w is 0.75 mm as shown in Fig.2 (a). From Equ.1, it is understandable that the capacitance of the sensor varies with humidity since the dielectric constant of paper is humidity dependent. Measurement of relative humidity of the environment is facilitated by the porous nature of cellulose paper which resulting in adsorption and desorption of water vapours [39].

The present sensor was realised through low cost manual screen printing technique. Fabrication process involves an aluminium frame holding a stretched polyester mesh of dimension 12 x 10 inches tightly with a thread count of 61 threads

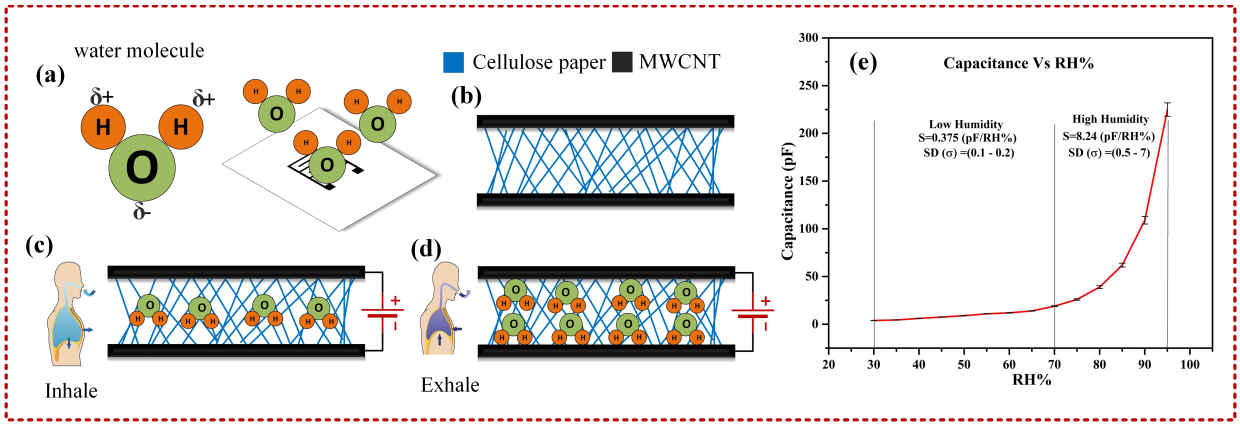


Fig. 3. Schematic representation of (a) interaction of water molecules with paper based humidity sensor, (b) porous cellulose structure of paper, interaction of water molecules with paper surface during (c) Inhalation and (d) exhalation influencing the capacitance changes and (e) Variation of capacitance of the paper based humidity sensor versus relative humidity.

per inch (TPI). A mask was formed over the mesh using a 20 $\mu$m capillary film emulsion and is dried in a dark place for one hour after coating. Mask for the sensor layout was created using CorelDraw design tool and a high-resolution print out was taken on a transparent sheet. Both the transparent sheet and the emulsion coated mesh were kept directly in contact with each other and exposed to 380 nm ultraviolet light for 45sec. Water was splashed thereafter on the screen to make the sensor patterns become visible. The screen was then loaded with MWCNT/PDMS composite as prepared earlier to print the sensor pattern on the photo paper substrate of thickness 130 $\mu$m. A 45° contact angle was retained between the squeegee and the screen. The screen printed MWCNT/PDMS composite was finally dried at 120°C for 60 min as displayed in Fig.2 (c-e).Furthermore, the prepared composite with different MWCNT ratio of 1%, 3%,5% and 6% by weight was examined for its printability and it was observed that higher filler ratio delivers highly conductive composite. 5% of MWCNT composite was found to be most optimal for the present printing process delivering smooth patterns and possessing better conductivity. Increasing the MWCNT concentration beyond 5% resulted in much higher viscosity of the composite reducing its flow through the mesh pores to the underlying substrate during screen printing process, thus affecting device printability. In addition, the composite also loses the physical bonding of the material with the substrate as well as its flexibility. The Scanning Electron Microscopy (SEM)(Carl Zeiss EVO / 18 Research) characterisation of the 5% MWCNT loaded composite film and paper substrate was also performed as shown in Fig.2 (f-g). The SEM image of the paper substrate in Fig.2 (h) shows a randomly oriented network of cellulose fibres and the porosity of the paper. The Energy Dispersive X-Ray (EDX) analysis was also done to ascertain the elemental compositions as shown in Fig.2 (i).

### C. Sensing Principle Measurement Technique

The present paper-based sensor utilizes the hygroscopic characteristics of cellulose paper which can adsorb water from the atmosphere. At a 70% RH, the paper adsorbs water up to 10% of its weight. The ionic conductivity of the paper is proportional to the amount of surface water in cellulose fibres, indicating a moisture content which is used as a principle to monitor respiration during breathing. During exhalation, human breath is completely humidified with 100% RH, and therefore, the amount of water on the sensor increases which in turn increases its ionic conductivity[48]. During inhalation process, the amount of surface water on the cellulose fibres is decreased since the surrounding environment almost always has a lower RH than the exhaled air. This reduction in the amount of adsorbed water reduces the ionic conductivity of the paper. Thus, during the breathing process, changes in the ionic conductivity alters the dielectric property of the paper due to the alteration in the amount of water molecules in the breath forming hydrogen bonding with polar -OH groups present on cellulose fibres as shown in Fig.3 (a-d). This variation in effective dielectric constant D forms the basis of measurement of a humidity sensor through changes in the output sensor capacitance C between the interdigitated electrodes as shown in Equ.3.The other parameters $\epsilon_0$ permittivity of dielectric, A sensing area and d distance between electrodes were remaining constant.

$$C = \frac{D\epsilon_0 A}{d} \tag{3}$$

Traditional humidity-sensing properties of the sensor were investigated initially by a simple relative humidity measuring system as shown in Fig.3 (e). The paper-based humidity sensor was exposed to RH varying from 30% to 95%, in steps of 5% RH, at a room temperature in a custom build humidity chamber. The chamber was also equipped with a DHT11 standard humidity and temperature sensor interfaced with Arduino data acquisition (DAQ) system to control, monitor, record and report the environmental data.

### D. Monitoring of Various Breathing Patterns

The experimental setup to investigate the response of the printed breath sensor towards variable breath conditions is shown in Fig.4. Fig.4(a) shows the schematic of the fabricated paper based breath sensor interfaced with Fluke 8846A

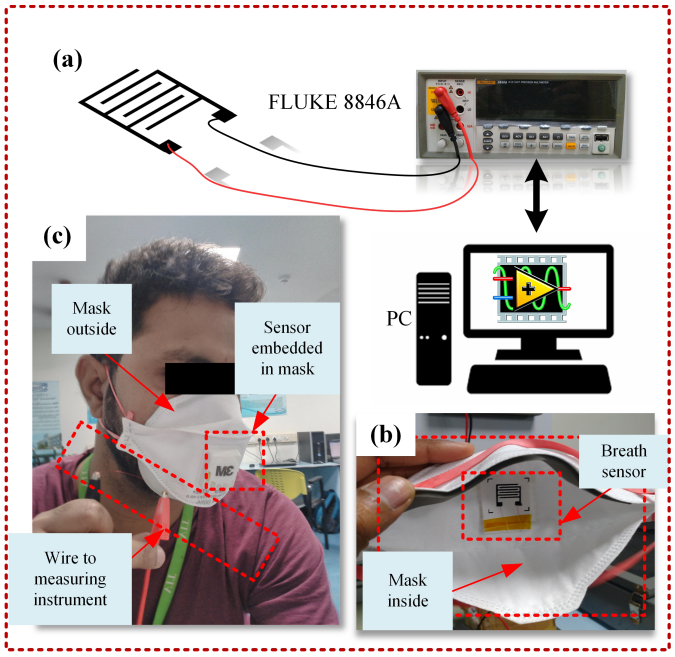


Fig. 4. (a) Schematic representation of the sensor connected with measuring instrument and PC, (b) Embedded sensor inside the mask and (c) The subject wearing the sensor embedded mask for testing.

precision digital multimeter, controlled by LabVIEW program was used for data logging and monitoring the respiration rate and its patterns. The sensor is attached near the philtrum and embedded inside a safety mask using a double-sided tape as shown in Fig.4 (b). A 3M 9332 Aura Disposable Respirator mask was used because of its low cost and extensive availability. Electrical connections to the printed sensor were made using the carbon conductive adhesive. Using a standard humidity and temperature sensor (DHT11), it was identified that the humidity and temperature in the mask varied between 75% – 95% and 32°C – 34.5°C respectively for the duration of breathing. Further since the environmental relative humidity in the current location varies between 55-60% and is significantly lower than the measurement range, along with the fact that the sensor is embedded inside a mask in a closed ambiance, the effect of seasonal or environmental variation would be negligible. The fabricated breath sensor mounted mask was tested with a healthy adult volunteer to evaluate the sensor performance in retrieving the breathing data under different breathing conditions as shown in Fig.4 (c). All the below experimental readings were performed for at least 5 times to account for the repeatability of the sensor and the plotted graphs shows mean and standard deviation for the data sets. Paper based similar breath sensors also shows insensitivity towards other exhaled gases like $CO_2$ primarily due to its very low solubility in water vapour [39] thereby demonstrating high selectivity of the sensor towards changes in humidity only. Fig.5 (a-b) shows the sensor mounted mask being tested initially for normal and deep breathing over a healthy individual to identify the efficacy of the sensor over different inhalation and exhalation capacities which forms a key parameter in various breathing abnormalities. The sensor was thereafter tested to identify differences between oral and nasal breathing for

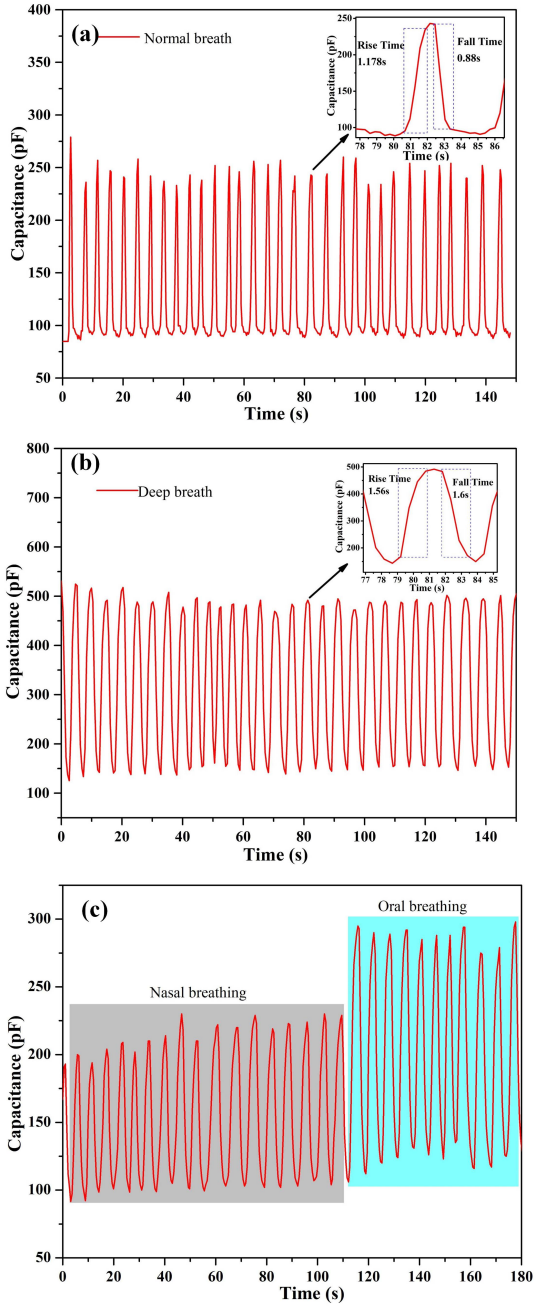


Fig. 5. Variation in sensor capacitance with breathing time for (a) normal breathing condition (b) deep breathing condition and (c) nasal and oral breathing conditions.

preliminary screening of improper breathing related health disorders like snoring and obstructive sleep apnea. Nasal breathing is well recognized to providing various benefits compared to oral breathing. The nose is outfitted with a sophisticated filtering mechanism to purify the breathing air before it entering lungs [49]. Swift *et al.* findings reported that the resistance to expiration provided by the nose helps maintain lung volumes and can be reflected in arterial oxygenation determination [50]. Habitual breathing through mouth makes an individual breath frequently in and out for continuous time periods and over regular intervals while taking rest or sleeping. It is well recorded that mouth breathing adults are more likely to be subjected to

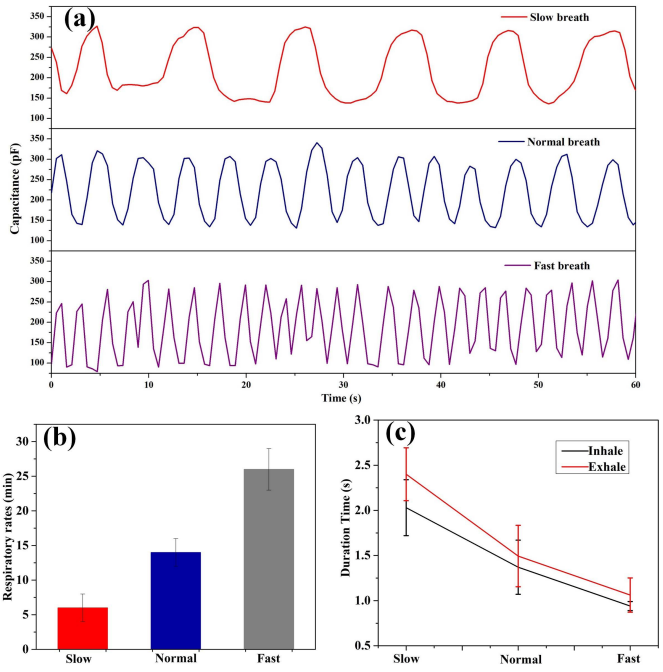


Fig. 6. (a) Variation in capacitance for three modes of respiration patterns recorded by sensor: Slow breath,Normal breath and Fast breath (b) Corresponding respiratory rates in three modes and (c) duration of the inhalation process and exhalation process in the three modes.

various sleep disorders, fatigue, and poor quality of life than those who practice nasal breathing [51], [52]. In the present study the subject underwent normal breathing through nose for about 2 minutes followed by normal breathing through mouth (oral breathing) for another 1 minute while wearing the sensor mounted mask as shown in Fig.5 (c).

A healthy adult normally breathes 12 to 20 times per minute with 6-8 L of air exchange[11]. For those with serious illnesses, a respiration rate higher than 24 breaths per minute indicates high risk [8]. For example, patients who suffer from severe infections or trauma might possess normal blood pressure, but with inappropriate heart beat resulting in a cardiac arrest [9]. In this situation, the rise in the respiration rate is regarded as an accurate sign of serious illness. Respiration failure is hard to predict and slow to recover, and can even create a life-threatening situation. Thus, continuous inspection on respiration is absolutely significant for use as a potential diagnostic device under such conditions. The breath sensor was tested for different respiration rates like (slow, normal, fast) as observed in Fig.6. Slow breathing, also identified as bradypnea, refers to breathing at a rate less than 12 breath/min for adults and is generally observed under sleeping condition. Under relaxed state, normal breathing rate is 12-20 breath/min for a healthy adult, whereas during hyperventilation or over breathing such as during a panic attack, after an exercise or after metabolic acidosis, the breathing rate becomes higher than 24 breath/min due to increased oxygen demand [53]. The above breathing patterns were recorded for the healthy subject under sleeping conditions for slow breathing, under a relaxed sitting position for normal breathing and while performing strenuous exercise for fast breathing or respiration rate.

The respiration rate (RR) or the number of beats per minute (bpm) was also monitored in addition to the depth rate (DR) or amplitude levels of the signal also for the subject under study after a light exercise (like walking) and after a heavy exercise (like climbing stairs). The obtained data was thereafter used to obtain the breathing index (BI) of the individual [39]. Finally, the sensor was then integrated with an Arduino unit to make a real time respiration monitoring unit.

## III. Result and Discussion

Variation in the capacitance of paper-based breath sensor for an initial testing of RH from 30%–95% at room temperature is presented in Fig.3 (c). It was observed that for lower humidity region, i.e. between 30-70%, the sensitivity of the sensor was relatively low at around 0.375 pF/RH%. However, for higher RH region of 70-95%, the sensitivity of the sensor enhances drastically and reaches to almost 8.24 pF/RH%. The above observation might be attributed to the change in the ionic conduction into the paper caused by the different concentration of adsorbed water molecules, which in turn varies the dielectric constant of the paper and subsequently the overall capacitance of the device with changing humidity level around them. For lesser humidity region the ionic conduction of the net adsorbed water molecules is extremely low showing a gradual change at the lower humidity range (30-70 RH%), but for higher humidity level, the density of water molecule adsorbed by the paper raises sharply resulting in a substantial rise above 70 RH%. This indicates that the response of the humidity sensor is nonlinear within the entire range (30-95 RH%) with a higher sensitivity beyond 70 RH%. However, although the paper based humidity sensor has no evident response to the RH below 70%, it can still fulfil the purpose of the human breath monitoring sensor as respiration activities mostly results in ambient RH greater than 70% [41], [39].

Monitoring of different breathing conditions was done on a healthy adult volunteer to study the feasibility of the sensor performance. During the breathing cycle, the sensor was exposed to varying levels of humidity in the inhaled and exhaled breathing. The observed capacitance curves indicated higher value of capacitance during exhalation whereas a lower value during inhalation time as explained earlier. Fig.5(a) shows the sensor capacitance output when tested under normal breathing and deep breathing conditions and exhibited significant differences. In the normal breathing cycle, the minimum capacitance of the sensor was observed to be $\sim$ 250 pF during exhalation and $\sim$ 100 pF during inhalation with net change in capacitance of $\sim$ 150 $\pm$ 20pF.The sensor rise time and fall time for normal breathing condition was observed to be $\sim$1.178s and 0.88s respectively. On the other hand deep breathing indicated a relatively higher minimum and maximum capacitance value of $\sim$ 150 pF during inhalation and $\sim$ 500 pF during exhalation respectively with a net change in capacitance of $\sim$ 350 $\pm$ 20 pF and larger rise and fall time of $\sim$1.56s and 1.6s as highlighted in Fig.5 (b). The above observation may be attributed to the significantly large volume of air movement during the deep breathing process. This increased quantity of moisture caused an increase in the values of the dielectric constant resulting in higher minimum and maximum

capacitance values in both inhaled and exhaled deep breath. This significant difference between normal and deep breathing suggests the applicability of the fabricated breath sensor for identification and diagnosis of several health conditions such as asthma, tachypnoea, etc. [54].

The fabricated sensor was also analysed for its performance under different breathing modes viz nasal and oral tract for preliminary screening of various breathing disorders. Fig.5(c) shows the observed response from the nasal and oral breathing taken for around 120s and 60s respectively. It was observed that the net capacitance of the sensor increases during oral breathing as compared to nasal breathing with a higher minimum and maximum capacitance values. Normal nasal breathing varied from ∼95 ± 10 pF to ∼230 ± 10 pF with a change in capacitance of ∼135 ± 10 pF similar to the previous experiment whereas the capacitance for oral breathing varied from ∼125 ± 10 pF upto ∼290 ± 10 pF with ΔC of ∼165 ± 20 pF. The increase in capacitance in case of oral breath is attributed to the large intakeof air volume and subsequent increase in number of molecules interacting with the sensor as compared to that of the nasal breath. Furthermore, presence of nasal mucosa creates filtered air which may also affect the overall capacitance during the nasal breathing mode.

The fabricated sensor was thereafter used for continuous inspection on respiration rate (RR) as discussed earlier. The response curves of the humidity sensor for various breathing rates are demonstrated in Fig.6 (a). The breath rate was manually counted for 60s by noting the peaks in the obtained graphs. Fig.6 (b) shows the plot of different respiration rate in slow, normal, and fast modes and were observed to be 6,14 and 26 per minute, respectively for the healthy subject as recommended, clearly indicating that the sensor could efficiently distinguish between varying breathing rates. Fig.6 (c) is obtained from the individual respiration process data for the three modes shown in Fig.6 (a). It was observed that the duration of inhaling duration in the slow, normal and fast modes are 2.03s,1.37s and 0.94s, while the exhaling duration was relatively more in the three modes as 2.4s,1.49s and 1.06s, respectively. Thus the paper-based breath sensor provided significant results on the respiration rate data, demonstrating its potential for real time health monitoring.

The breathing rate was also monitored for a different subject after light walking and climbing six floors and breathing index (BI) was calculated to estimate the fitness level of the individual. It was observed that when the task was changed from light exercise to a vigorous exercise, both respiration rates (RR) and the amplitude levels of the signals i.e. depth rates (DR) changes. DR is calculated based on the capacitance change in every respiration state. Breathing index (*BI*) is defined as the ratio of breath rate to the peak-to-peak breath amplitude under light and vigorous exercises and is given by Equ.4 as following [39], [55]:

$$BI = \left(\frac{DR_{vigorous}}{DR_{light}}\right) \times \left(\frac{RR_{vigorous}}{RR_{light}}\right) \tag{4}$$

where, DR*vigorous* and RR*vigorous* signify the depth and breath rate of respiration during vigorous exercise and

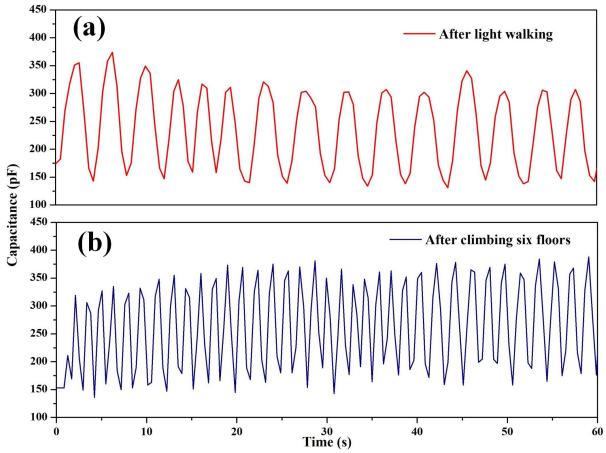


Fig. 7. Respiration patterns showing change in capacitance values of second test subject (a) after light walking and (b) after climbing six floors.

DR*light* and RR*light* signify the depth and respiration rate during light exercise.

Owing to faster breath rate and the heavy depth of respiration, the patterns observed could be easily recognized as shown in Fig.7. It was observed that changes in the DR were not very significant during light or vigorous exercise. This may be attributed to the fact that DR depends upon the tidal volume of the lungs which in turn depends upon the metabolic demand and increases after a light or vigorous exercise [56]. Consequently, DR remains an insignificant part in calculation of BI. The RR on the other hand is attributed by changes in respiratory frequency and is accountable to the physical effort provided during light or vigorous exercise [57]. For fit individuals RR under vigorous exercise thus won't significantly increase (i.e. much physical effort is not required) similar to that during lighter exercise as compared to that for an unfit individual. Thus, breathing index for fit individuals remain close to unity [39], [55], whereas, unfit individuals have higher BI primarily due to increased RR ratio. In the present case, the RR or the number of beats per minute (bpm) after light walking was 15 while that after climbing six floors was 36. In addition, the amplitude of the signal (ΔC) changes from ∼135 ± 20 pF in normal breathing condition to ∼190 ± 50 pF after exercise as also depicted in figure 8(b). Thus according to Equ 4, the BI was estimated to be approximately 3.37 (>3) as shown below:

$$BI = \left(\frac{190pF}{135pF}\right) \times \left(\frac{36RR}{15RR}\right) = 3.37 \tag{5}$$

The above result may thus suggest that the subjects' respiration frequency changed significantly indicating the individual to be not very fit with increased BI of 3.37 [39].

Considering the current pandemic situation, wearing a facial mask has become a need of the hour. Further, monitoring of respiratory rate (RR), and its normalization under resting condition has become one of the most significant sign to identify clinical recovery from COVID-19 infection [58]. In this context, periodic short-term screening or continuous monitoring of RR for persons with varying symptoms is in great demand and becomes more significant change for

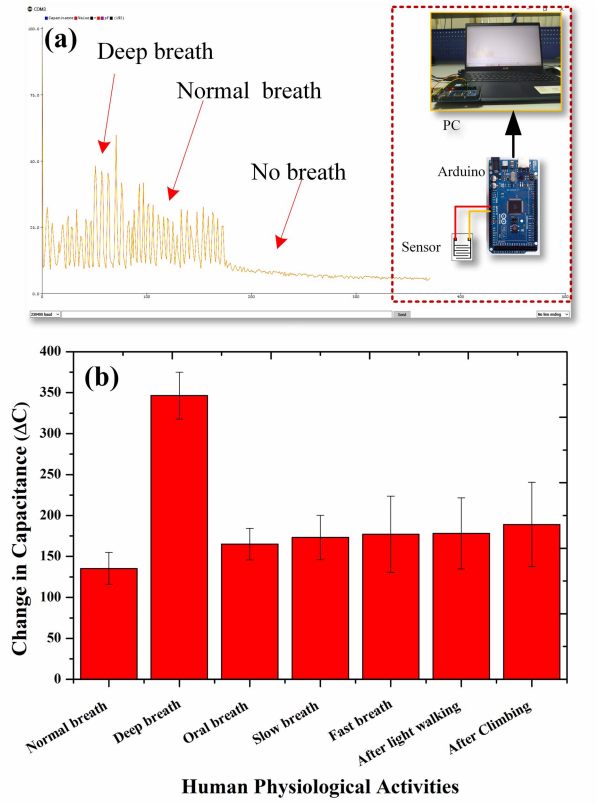


Fig. 8. (a) Schematic illustration of Arduino based breath monitoring system (b) Changes in capacitance values for different physical activities with their standard deviation recorded for multiple data sets.

persons being monitored remotely from distant places. Additionally, high sensitivity, low cost and potential application of the present sensor integrated inside a facial mask might aid the development of the much needed smart masks for real time monitoring of breath patterns. In this regard a low cost and portable data acquisition system for patient monitoring was also developed with the help of Arduino circuit board as shown in Fig.8 (a) integrated with the smart sensor embedded mask. The embedded breath sensor was connected to the analog pins and the microcontroller program was tuned to time constant (TC) of the sensor in seconds, as TC=R*C for measuring the capacitance of the sensor where TC corresponds to 63.2% of the peak value. The developed hardware system was thus capable of acquiring the breath signals from the subjects, and clearly identifying different breathing patterns making a real time respiration monitoring system as well as a preliminary diagnostic tool for potential health seekers.

The current paper-based breath sensor shows good response towards detection of breath parameters during myriad of physical activities. Fig.8 (b) distinctly presents the change in capacitance ($\Delta C$) for different physical activities monitored above. The capacitance change for normal breathing was the mean of various normal modes as shown in Fig.5 (a), Fig.6 (a) and nasal breath of Fig.5 (c) and is regarded as the standard for comparison. It was observed that deep breath creates highest change in capacitance due to large exchange of air volume and corresponding water vapour molecules. Similarly, oral breathing showed larger capacitance change with greater irregularities on similar accounts indicating breathing irregularities. Significant difference in $\Delta C$ between slow and fast breathing was not observed both the processes involve intake and release of relatively larger air volumes than normal with major difference being in the time taken for each breathing cycle. Finally, it was observed that mild to heavy exercise, both resulted in relatively larger $\Delta C$ as compared to normal breathing indicating larger tidal volume due to increased metabolic demand during an exercise as compared to that under normal condition [56] with $\Delta C$ being almost same for mild (walking) or vigorous exercise (climbing) while only the respiratory frequency changed during the exercise. These significant changes in $\Delta C$ along with their deviation might not only prove to be of highly informative diagnostic tool in the hands of clinicians to predict breathing disorders as well as respiration rate abnormalities but also for other multifunctional applications like measurement of dehydration levels in infants, diaper wetness levels for infants and elderly people suffering from urinary incontinence, monitoring of RH distribution, etc [41], [59].

## IV. Conclusion

Breath monitoring of patients can be a useful technique to assess the health condition of patients. With overgrowing respiratory problems like asthma, pneumonia, and COVID-19 this technique could pave an easy, simple, and non-invasive real time technique of monitoring respiratory patterns. Present study discusses the design, fabrication, and characterization of a wearable capacitive humidity sensor for respiration monitoring system. The sensor in this study was fabricated using conventional screen printing of multi-walled carbon nanotubes (MWCNT) and polydimethylsiloxane (PDMS) composite in the form of interdigitated electrodes on a paper substrate. The 5wt% MWCNT composite was found to exhibit good printability as well as conductivity on a commercial photo printing paper. The hygroscopic nature of the paper effectively converted the humidity changes into dielectric constant changes of the paper during inhalation and exhalation, with subsequent changes in sensor capacitance. The configuration of composite interdigitated electrodes indicated high sensitivity of almost 8.24 pF/Rh% for humidity levels above 70% and a good response time of 1.178s rise time under exhalation periods and 0.88s as the inhalation fall time when examined using human subjects under normal breathing conditions. The sensor demonstrated good distinction between different breathing conditions like normal and deep breathing with a high change in capacitance of $\sim$ 350 $\pm$ 20 pF for deep breathing as compared to a capacitance of $\sim$150 $\pm$ 20pF for normal breathing owing to high water vapour content and dielectric change during deep breathing period. Similarly, oral breathing and fast breathing demonstrated a large capacitance levels for the same reason and showed relatively large variation compared to normal breathing highlighting a potentially important parameter for diagnosis of abnormal breath parameters. Efficacy of the sensors were further tested by measuring the respiration rates (RR) under different conditions and were observed to be 6, 14 and 26 per minute, respectively for the healthy subject under slow, normal and fast breathing.

Similarly, RR obtained after light walking was 15 compared to 36 after climbing six floors. Additionally, the amplitude of the breath's i.e. depth rate (DR) changed quickly before and after the exercise which form important parameters for measurement of breathing index and several others. Thus deployment of the sensor in the wearable mask proved to be highly effective in monitoring and distinguishing various breathing responses as indicated through Fig.8 (b) towards normal breathing, deep breathing, workout, oral, fast and slow breath, etc integrated with a real time portable monitoring system. This strategy is also identified to possess good sensitivity, biodegradability and stability to serve tremendously in the wearable and flexible healthcare field as a smart mask highlighting the efficacy and need during the current pandemic situation and for the moments to come.

## ACKNOWLEDGMENT

The authors would like to thank Keetronics (India) Pvt. Ltd., Pune, for providing printing facility and useful discussions. They also like to thank the Vellore Institute of Technology, Vellore, for facilitating the sensor characterisation laboratory.

## REFERENCES

[1] M. Ha, S. Lim, and H. Ko, "Wearable and flexible sensors for user-interactive health-monitoring devices," *J. Mater. Chem. B*, vol. 6, no. 24, pp. 4043–4064, 2018, doi: 10.1039/c8tb01063c.

[2] X. Wang, Z. Liu, and T. Zhang, "Flexible sensing electronics for wearable/attachable health monitoring," *Small*, vol. 13, no. 25, pp. 1–19, 2017, doi: 10.1002/smll.201602790.

[3] D. Maji and S. Das, "Simulation and feasibility study of flow sensor on flexible polymer for healthcare application," *IEEE Trans. Biomed. Eng.*, vol. 60, no. 12, pp. 3298–3305, Dec. 2013, doi: 10.1109/TBME.2013.2265319.

[4] Y. Huang *et al.*, "High-resolution flexible temperature sensor based graphite-filled polyethylene oxide and polyvinylidene fluoride composites for body temperature monitoring," *Sens. Actuators A, Phys.*, vol. 278, pp. 1–10, Aug. 2018, doi: 10.1016/j.sna.2018.05.024.

[5] C.-C. Yeh, S.-H. Lo, M.-X. Xu, and Y.-J. Yang, "Fabrication of a flexible wireless pressure sensor for intravascular blood pressure monitoring," *Microelectron. Eng.*, vol. 213, pp. 55–61, May 2019, doi: 10.1016/j.mee.2019.04.009.

[6] H.-H. Jang, J.-S. Park, and B. Choi, "Flexible piezoresistive pulse sensor using biomimetic PDMS mold replicated negatively from shark skin and PEDOT:PSS thin film," *Sens. Actuators A, Phys.*, vol. 286, pp. 107–114, Feb. 2019, doi: 10.1016/j.sna.2018.12.015.

[7] S. K. Kundu, S. Kumagai, and M. Sasaki, "A wearable capacitive sensor for monitoring human respiratory rate," *Jpn. J. Appl. Phys.*, vol. 52, no. 4S, Apr. 2013, Art. no. 04CL05, doi: 10.7567/JJAP.52.04CL05.

[8] P. B. Lovett, J. M. Buchwald, K. Stürmann, and P. Bijur, "The vexatious vital: Neither clinical measurements by nurses nor an electronic monitor provides accurate measurements of respiratory rate in triage," *Ann. Emergency Med.*, vol. 45, no. 1, pp. 68–76, Jan. 2005, doi: 10.1016/j.annemergmed.2004.06.016.

[9] M. Grassmann, E. Vlemincx, A. Von Leupoldt, J. M. Mittelstädt, and O. Van den Bergh, "Respiratory changes in response to cognitive load: A systematic review," *Neural Plasticity*, vol. 2016, no. 5, pp. 1–16, Jan. 2016, doi: 10.1155/2016/8146809.

[10] S. D. Min, Y. Yun, and H. Shin, "Simplified structural textile respiration sensor based on capacitive pressure sensing method," *IEEE Sensors J.*, vol. 14, no. 9, pp. 3245–3251, Sep. 2014, doi: 10.1109/JSEN.2014.2327991.

[11] O. Atalay, W. R. Kennon, and E. Demirok, "Weft-knitted strain sensor for monitoring respiratory rate and its electro-mechanical modeling," *IEEE Sensors J.*, vol. 15, no. 1, pp. 110–122, Jan. 2015, doi: 10.1109/JSEN.2014.2339739.

[12] G. Tardi, C. Massaroni, P. Saccomandi, and E. Schena, "Experimental assessment of a variable orifice flowmeter for respiratory monitoring," *J. Sensors*, vol. 2015, pp. 1–7, Jul. 2015, doi: 10.1155/2015/752540.

[13] Y. Liu *et al.*, "Epidermal electronics for respiration monitoring via thermo-sensitive measuring," *Mater. Today Phys.*, vol. 13, Jun. 2020, Art. no. 100199, doi: 10.1016/j.mtphys.2020.100199.

[14] J. Grlica, T. Martinović, and H. Džapo, "Capacitive sensor for respiration monitoring," in *Proc. IEEE Sensors Appl. Symp. (SAS)*, Apr. 2015, pp. 1–6, doi: 10.1109/SAS.2015.7133567.

[15] S. W. Park, P. S. Das, A. Chhetry, and J. Y. Park, "A flexible capacitive pressure sensor for wearable respiration monitoring system," *IEEE Sensors J.*, vol. 17, no. 20, pp. 6558–6564, Oct. 2017, doi: 10.1109/JSEN.2017.2749233.

[16] L. Guidetti, M. Meucci, F. Bolletta, G. P. Emerenziani, M. C. Gallotta, and C. Baldari, "Validity, reliability and minimum detectable change of COSMED K5 portable gas exchange system in breath-by-breath mode," *PLoS ONE*, vol. 13, no. 12, pp. 1–12, 2018, doi: 10.1371/journal.pone.0209925.

[17] D. N. Dutta, R. Das, and S. Pal, "Automated real-time processing of single lead electrocardiogram for simultaneous heart rate and respiratory rate monitoring," *J. Med. Device*, vol. 11, no. 2, pp. 1–9, Jun. 2017, doi: 10.1115/1.4035982.

[18] H. R. W. Touw *et al.*, "Photoplethysmography respiratory rate monitoring in patients receiving procedural sedation and analgesia for upper gastrointestinal endoscopy," *J. Clin. Monitor. Comput.*, vol. 31, no. 4, pp. 747–754, Aug. 2017, doi: 10.1007/s10877-016-9890-0.

[19] M. Folke, L. Cernerud, M. Ekström, and B. Hök, "Critical review of non-invasive respiratory monitoring in medical care," *Med. Biol. Eng. Comput.*, vol. 41, no. 4, pp. 377–383, Jul. 2003, doi: 10.1007/BF02348078.

[20] J. LaWall, "Sleep medicine: A guide to sleep and its disorders," *J. Clin. Sleep Med.*, vol. 2, no. 3, p. 365, 2006, doi: 10.5664/jcsm.26603.

[21] C. Massaroni, A. Nicolò, D. Lo Presti, M. Sacchetti, S. Silvestri, and E. Schena, "Contact-based methods for measuring respiratory rate," *Sensors*, vol. 19, no. 4, pp. 1–47, 2019, doi: 10.3390/s19040908.

[22] G. Wang *et al.*, "Fast-response humidity sensor based on laser printing for respiration monitoring," *RSC Adv.*, vol. 10, no. 15, pp. 8910–8916, Mar. 2020, doi: 10.1039/c9ra10409g.

[23] J. E. Ellis and A. Star, "Carbon nanotube based gas sensors toward breath analysis," *ChemPlusChem*, vol. 81, no. 12, pp. 1248–1265, Dec. 2016, doi: 10.1002/cplu.201600478.

[24] J. He *et al.*, "High performance humidity fluctuation sensor for wearable devices via a bioinspired atomic-precise tunable graphene-polymer heterogeneous sensing junction," *Chem. Mater.*, vol. 30, no. 13, pp. 4343–4354, Jul. 2018, doi: 10.1021/acs.chemmater.8b01587.

[25] M. Righettoni, A. Amann, and S. E. Pratsinis, "Breath analysis by nanostructured metal oxides as chemo-resistive gas sensors," *Mater. Today*, vol. 18, no. 3, pp. 163–171, Apr. 2015, doi: 10.1016/j.mattod.2014.08.017.

[26] N. Li, X.-D. Chen, X.-P. Chen, X. Ding, and X. Zhao, "Ultra-high sensitivity humidity sensor based on $MoS_2$/Ag composite films," *IEEE Electron Device Lett.*, vol. 38, no. 6, pp. 806–809, Jun. 2017, doi: 10.1109/LED.2017.2699332.

[27] B. Li, G. Xiao, F. Liu, Y. Qiao, C. M. Li, and Z. Lu, "A flexible humidity sensor based on silk fabrics for human respiration monitoring," *J. Mater. Chem. C*, vol. 6, no. 16, pp. 4549–4554, 2018, doi: 10.1039/c8tc00238j.

[28] R. Xie *et al.*, "Wearable leather-based electronics for respiration monitoring," *ACS Appl. Bio Mater.*, vol. 2, no. 4, pp. 1427–1431, Apr. 2019, doi: 10.1021/acsabm.9b00082.

[29] S. Khan, L. Lorenzelli, and R. S. Dahiya, "Technologies for printing sensors and electronics over large flexible substrates: A review," *IEEE Sensors J.*, vol. 15, no. 6, pp. 3164–3185, Jun. 2015, doi: 10.1109/JSEN.2014.2375203.

[30] W. Wu, "Inorganic nanomaterials for printed electronics: A review," *Nanoscale*, vol. 9, no. 22, pp. 7342–7372, 2017, doi: 10.1039/c7nr01604b.

[31] S. Tong, J. Sun, and J. Yang, "Printed thin-film transistors: Research from China," *ACS Appl. Mater. Interface*, vol. 10, no. 31, pp. 25902–25924, Aug. 2018, doi: 10.1021/acsami.7b16413.

[32] Z. Chu, J. Peng, and W. Jin, "Advanced nanomaterial inks for screen-printed chemical sensors," *Sens. Actuator B, Chem.*, vol. 243, pp. 919–926, May 2017, doi: 10.1016/j.snb.2016.12.022.

[33] Y. Zhang *et al.*, "Flexible electronics based on micro/nanostructured paper," *Adv. Mater.*, vol. 30, no. 51, pp. 1–39, 2018, doi: 10.1002/adma.201801588.

[34] N. Colozza *et al.*, "A wearable origami-like paper-based electrochemical biosensor for sulfur mustard detection," *Biosensors Bioelectron.*, vol. 129, pp. 15–23, Mar. 2019, doi: 10.1016/j.bios.2019.01.002.

[35] T. K., G. K. Rajini, and D. Maji, "Paper-based screen printed MWCNT-PDMS composite strain sensor for human motion monitoring," in *Proc. IEEE 16th India Council Int. Conf. (INDICON)*, Dec. 2019, pp. 1–4, doi: 10.1109/indicon47234.2019.9030347.

[36] H. Liu, H. Jiang, F. Du, D. Zhang, Z. Li, and H. Zhou, "Flexible and degradable paper-based strain sensor with low cost," *ACS Sustain. Chem. Eng.*, vol. 5, no. 11, pp. 10538–10543, Nov. 2017, doi: 10.1021/acssuschemeng.7b02540.

[37] L. Gao *et al.*, "All paper-based flexible and wearable piezoresistive pressure sensor," *ACS Appl. Mater. Interface*, vol. 11, no. 28, pp. 25034–25042, Jul. 2019, doi: 10.1021/acsami.9b07465.

[38] X. Gong, L. Zhang, Y. Huang, S. Wang, G. Pan, and L. Li, "Directly writing flexible temperature sensor with graphene nanoribbons for disposable healthcare devices," *RSC Adv.*, vol. 10, no. 37, pp. 22222–22229, Jun. 2020, doi: 10.1039/d0ra02815k.

[39] F. Güder *et al.*, "Paper-based electrical respiration sensor," *Angew. Chem. Int. Ed.*, vol. 55, no. 19, pp. 5727–5732, May 2016, doi: 10.1002/anie.201511805.

[40] S. Kanaparthi, "Pencil-drawn paper-based non-invasive and wearable capacitive respiration sensor," *Electroanalysis*, vol. 29, no. 12, pp. 2680–2684, Dec. 2017, doi: 10.1002/elan.201700438.

[41] Z. Duan *et al.*, "Facile, flexible, cost-saving, and environment-friendly paper-based humidity sensor for multifunctional applications," *ACS Appl. Mater. Interface*, vol. 11, no. 24, pp. 21840–21849, Jun. 2019, doi: 10.1021/acsami.9b05709.

[42] J. Wala, D. Maji, and S. Das, "Influence of physico-mechanical properties of elastomeric material for different cell growth," *Biomed. Mater.*, vol. 12, no. 6, Oct. 2017, Art. no. 065002.

[43] J. Du *et al.*, "Optimized CNT-PDMS flexible composite for attachable health-care device," *Sensors*, vol. 20, no. 16, pp. 1–13, 2020.

[44] J. H. Kim *et al.*, "Simple and cost-effective method of highly conductive and elastic carbon nanotube/polydimethylsiloxane composite for wearable electronics," *Sci. Rep.*, vol. 8, no. 1, pp. 1–11, Dec. 2018, doi: 10.1038/s41598-017-18209-w.

[45] A. A. Chlaihawi, B. B. Narakathu, S. Emamian, B. J. Bazuin, and M. Z. Atashbar, "Development of printed and flexible dry ECG electrodes," *Sens. Bio-Sens. Res.*, vol. 20, pp. 9–15, Sep. 2018, doi: 10.1016/j.sbsr.2018.05.001.

[46] S. Y. Madani, A. Mandel, and A. M. Seifalian, "A concise review of carbon nanotube's toxicology," *Nano Rev.*, vol. 1, pp. 1–14, Jan. 2013.

[47] J. Oberländer *et al.*, "Study of interdigitated electrode arrays using experiments and finite element models for the evaluation of sterilization processes," *Sensors*, vol. 15, no. 10, pp. 26115–26127, Oct. 2015, doi: 10.3390/s151026115.

[48] R. J. Moon, A. Martini, J. Nairn, J. Simonsen, and J. Youngblood, "Cellulose nanomaterials review: Structure, properties and nanocomposites," *Chem. Soc. Rev.*, vol. 40, no. 7, pp. 3941–3994, 2011.

[49] R. Fried, "The hyperventilation syndrome-research and clinical treatment," *J. Neurol., Neurosurg. Psychiatry*, vol. 51, no. 12, pp. 1600–1601, Dec. 1988, doi: 10.1136/jnnp.51.12.1600-b.

[50] D. M. Ludlum, "January 1988," *Weatherwise*, vol. 41, no. 2, pp. 119–123, 1988, doi: 10.1080/00431672.1988.9925259.

[51] M. Lunn and T. Craig, "Rhinitis and sleep," *Sleep Med. Rev.*, vol. 15, no. 5, pp. 293–299, Oct. 2011, doi: 10.1016/j.smrv.2010.12.001.

[52] J. Mullol, M. Maurer, and J. Bousquet, "Sleep and allergic rhinitis," *J. Invest. Allergol. Clin. Immunol.*, vol. 18, no. 6, pp. 415–419, 2008.

[53] J. Wang, S. Soltanian, P. Servati, F. Ko, and M. Weng, "A knitted wearable flexible sensor for monitoring breathing condition," *J. Eng. Fibers Fabrics*, vol. 15, 2020, Art. no. 1558925020930354.

[54] A. T. Güntner, S. Abegg, K. Königstein, P. A. Gerber, A. Schmidt-Trucksäss, and S. E. Pratsinis, "Breath sensors for health monitoring," *ACS Sensors*, vol. 4, no. 2, pp. 268–280, Feb. 2019, doi: 10.1021/acssensors.8b00937.

[55] V. Balakrishnan *et al.*, "Paper-based electronics using graphite and silver nanoparticles for respiration monitoring," *IEEE Sensors J.*, vol. 19, no. 24, pp. 11784–11790, Dec. 2019, doi: 10.1109/JSEN.2019.2939567.

[56] A. Nicolò and M. Sacchetti, "A new model of ventilatory control during exercise," *Exp. Physiol.*, vol. 104, no. 9, pp. 1331–1332, Sep. 2019, doi: 10.1113/EP087937.

[57] A. Nicolò, C. Massaroni, and L. Passfield, "Respiratory frequency during exercise: The neglected physiological measure," *Frontiers Physiol.*, vol. 8, pp. 1–8, Dec. 2017, doi: 10.3389/fphys.2017.00922.

[58] C. Massaroni, A. Nicolò, E. Schena, and M. Sacchetti, "Remote respiratory monitoring in the time of COVID-19," *Frontiers Physiol.*, vol. 11, pp. 1–4, May 2020, doi: 10.3389/fphys.2020.00635.

[59] U. Mogera, A. A. Sagade, S. J. George, and G. U. Kulkarni, "Ultrafast response humidity sensor using supramolecular nanofibre and its application in monitoring breath humidity and flow," *Sci. Rep.*, vol. 4, no. 1, pp. 1–9, May 2015, doi: 10.1038/srep04103.


**K. Thiyagarajan** (Student Member, IEEE) received the M.Tech. degree in control and automation from the Vellore Institute of Technology (VIT), Vellore, in 2016, where he is currently pursuing the Ph.D. degree with the School of Electrical Engineering. His research interests include nanomaterials, printed electronics, and flexible sensors.

**G. K. Rajini** (Member, IEEE) received the master's degree in sensors systems technology from the Vellore Institute of Technology (VIT), Vellore, India, in 2005, and the Ph.D. degree from Sri Venkateswara University, Tirupati, India, in 2016. Since July 2011, she has been working as an Associate Professor with the Vellore Institute of Technology (VIT). She has 25 years of teaching expereince and four years of industrial expereince. Her research interests include signal processing, bio medical sensors, biosignal processing, and digital image processing.

**Debashis Maji** (Member, IEEE) received the M.Tech. degree in sensor system technology from the Vellore Institute of Technology (VIT), Vellore, India, and the Ph.D. degree in the interdisciplinary area of BioMEMS and Flexible Sensors from the School of Medical Science and Technology, Indian Institute of Technology, Kharagpur. He is currently working as a Senior Assistant Professor with the Department of Sensor and Biomedical Technology, School of Electronics Engineering (SENSE), Vellore Institute of Technology (VIT). His research interests include design and fabrication of thin and thick film based flexible biosensors, BioMEMS, and microfluidic biochips for biomedical applications. He is an active member for last ten years.